

Periodic Time-Domain Nonlocal Nonreflecting Boundary Conditions for Duct Acoustics

Willie R. Watson and William E. Zorumski
Langley Research Center, Hampton, Virginia

June 1996

National Aeronautics and
Space Administration
Langley Research Center
Hampton, Virginia 23681-0001

1 Introduction

In flow ducts, transient acoustic waves are rapidly dissipated by viscous forces that are present in all real flows. This phenomenon leaves the periodic sound as the dominate source of noise for most duct acoustics problems. Understanding the behavior of these periodic sound waves has long been an important goal in duct acoustics research. The importance of this goal has further increased as aircraft acoustic analyses have been required to include the effects of increasingly severe operating conditions. To date, most analytical research has used simplified frequency-domain models to obtain knowledge in regard to flow effects on periodic sound waves. However, the research community has generally accepted the fact that a fully adequate treatment of sound effects in flow ducts will be achieved only through a direct numerical solution to Euler equations. In this approach, periodic acoustic waves are obtained by integrating the Euler equations to a periodic state. Unfortunately, the absence of dissipation from these equations means that acoustic transients that are introduced when these fluid dynamics equations are integrated from a given initial state do not decay naturally as they do in reality. As a result, transient waves must be eliminated by other means so that the proper periodic state can be achieved.

One means for eliminating initial transients from a set of inviscid equations such as the Euler equations is to include artificial viscosity in the numerical scheme. However, the inclusion of the artificial viscosity often damps the acoustic disturbances so that the appropriate periodic steady state is not captured. The method often used to extract the periodic steady-state field from Euler's equations is to specify time-domain conditions on the boundary of the computational domain that guarantee that incident energy is not reflected. This subject was treated, for example, in references [1]-[6]. The computational boundary conditions that are presented in these works are local; and these boundary conditions are not generalizable to higher dimensions, arbitrary sound sources, and acoustically treated ducts.

In two recent papers (references [7, 8]), nonreflecting boundary conditions were shown to be obtainable in the frequency-domain by using nonlocal computational boundary conditions. The purpose of this paper is to extend these frequency-domain computational boundary conditions to the time domain. When nonreflecting frequency domain boundary conditions are applied in the time domain, they are not necessarily transparent to transient waves because, in time-domain computations, transient acoustic waves are introduced by the initial conditions. Thus, one issue that must be dealt with immediately in this context is the elimination of transient acoustic waves, which were absent in the frequency-domain analysis of the two earlier works (reference [7, 8]). Here, a set of time-domain computational boundary conditions that allow periodic waves to pass without reflecting is derived. These boundary conditions are referred to as periodic nonreflecting time-domain boundary conditions.

In the following section the physical duct acoustics problem, which is infinite in extent, is described and the initial boundary value problem is formulated. In section 3, the time-domain computational boundary-condition operators are presented. These boundary-condition operators allow the domain to be truncated to a finite length to achieve computational efficiency. These conditions are shown to be convolution integrals of the corresponding frequency-domain operators that are presented in reference [7]. In section 4, the boundary conditions are coupled to the Euler equations and advanced to a periodic state by using MacCormack's algorithm. Results for both a pure and a multitone source for several initial

conditions are given in section 5. Conclusions are given in section 6.

2 Problem Formulation

2.1 Rectangular Duct and Coordinate System

Consider a rectangular duct with the inflow and outflow boundary at $x = 0$ and $x = L$, respectively, as shown in figure 1. Although the duct is assumed to be infinitely long in the axial direction, the computational domain is limited to a finite length L , and the sound field is considered to be independent of the y direction (i.e., planar). The sound source is located at the inflow boundary and is assumed to be periodic in time with a fundamental period of, T . The sound source generates acoustic disturbances that propagate from left to right in the duct. Only compressible, inviscid disturbances without heat conduction are considered.

For purposes of this paper, the fluid in the duct is assumed to decompose into a background and an acoustic component. The background pressure P_0 , density ρ_0 , and temperature T_0 are constant. The background flow has zero velocity. The cross-sectional area of the duct is constant, although extension of the analysis to higher dimensions and variable-area ducts is straightforward. At time $t = 0$, the disturbance in the duct is assumed to be known. As is common in acoustics, the source pressure $g(t)$ is assumed to be known for all $t > 0$ and drives the flow. Finally, acoustic waves that exit the computational domain at $x = L$ do so without reflecting. The goal here is to derive time-domain nonreflecting boundary conditions that allow the duct to be terminated at $x = L$. These boundary conditions must also be capable of driving the system to a time-periodic state.

2.2 Governing Equations

The fundamental equations that govern inviscid compressible disturbances in the duct are the Euler equations (reference [9]):

$$\frac{\partial \{U\}}{\partial t} + \frac{\partial \{H\}}{\partial x} = \{0\} \quad (1)$$

$$\{U\} = \begin{Bmatrix} \rho \\ \rho u \\ E \end{Bmatrix} \quad (2)$$

$$\{H\} = \begin{Bmatrix} \rho u \\ (\rho u^2 + p) \\ (E + p)u \end{Bmatrix} \quad (3)$$

$$E = C_v T + \frac{u^2}{2} \quad (4)$$

where C_v is the specific heat at constant volume. Equation (1) is a vector equation that contains three components. Physically, the first, second, and third components represent the conservation of the mass, the x momentum, and the energy, respectively, within the duct. The unknown variables are the fluid density ρ , axial velocity u , temperature T , and pressure

p . Thus, the vector equation (1) is a system of three equations in four unknown variables ρ, p, T , and u . To close the system, an ideal gas is assumed:

$$p = \rho RT \quad (5)$$

Here, R is the universal gas constant. Equation (5) is used to eliminate temperature and to reduce the system to three equations in three unknown variables.

Equations (1)-(5) are the most general set of nonlinear fluid dynamic equations; these equations govern inviscid compressible disturbances in the duct. No known periodic solutions exist for these equations in this most general form. Therefore, the objective in direct numerical simulation is to numerically evolve these equations to a periodic state which requires the specification of initial and boundary conditions.

2.3 Initial and Boundary Conditions

As is common in initial boundary value problems in fluid dynamics, the flow will be initiated from a state of rest:

$$p(x, 0) = P_0 \quad (6)$$

$$\rho(x, 0) = \rho_0 \quad (7)$$

and

$$u(x, 0) = 0 \quad (8)$$

where P_0 and ρ_0 are constants. The governing equations require inflow and outflow boundary conditions. The Euler equations in one space dimension and time require two boundary conditions at the subsonic inflow and one condition at the subsonic outflow (reference [3]). At the inflow, the disturbance pressure is prescribed so that

$$p(0, t) = P_0 + g(t) \quad (9)$$

The inflow acoustic disturbance is assumed to be linear and homentropic:

$$\frac{\partial p(0, t)}{\partial x} - c_0^2 \frac{\partial \rho(0, t)}{\partial x} = 0 \quad (10)$$

Here, c_0 is the ambient speed of sound which is defined as

$$c_0^2 = \frac{\gamma P_0}{\rho_0} \quad (11)$$

where γ is the ratio of specific heats and is approximately equal to 1.4 for air at standard conditions. Finally, the initial boundary value problem is fully specified when a radiation condition is specified at the outflow boundary $x = L$. Development of the radiation condition is the subject of the following section.

3 Radiation Condition for Periodic Solutions

The radiation condition relates the acoustic pressure \tilde{p} and the normal component of acoustic velocity \tilde{u} at the outflow boundary $x = L$. The Fourier series for the periodic pressure and axial velocity can be given in complex form as

$$p(L, t) = P_0 + \tilde{p}(L, t) \quad (12)$$

$$u(L, t) = U_0 + \tilde{u}(L, t) \quad (13)$$

$$\tilde{p}(L, t) = \sum_{n=-\infty}^{\infty} \hat{p}(L; \omega_n) e^{i\omega_n t} \quad (14)$$

$$\tilde{u}(L, t) = \sum_{n=-\infty}^{\infty} \hat{u}(L; \omega_n) e^{i\omega_n t} \quad (15)$$

the frequency ω_n is defined in terms of harmonic number n and the fundamental period of the sound source T :

$$\omega_n = \frac{2n\pi}{T} \quad (16)$$

where n is an integer. The periodicity condition is

$$\tilde{p}(L, t + T) = \tilde{p}(L, t) \quad (17)$$

and

$$\tilde{u}(L, t + T) = \tilde{u}(L, t) \quad (18)$$

Band-limited periodic functions contain a finite number of terms $n \leq N$ such that

$$\tilde{p}(L, t) = \sum_{n=-N}^N \hat{p}(L; \omega_n) e^{i\omega_n t} \quad (19)$$

and

$$\tilde{u}(L, t) = \sum_{n=-N}^N \hat{u}(L; \omega_n) e^{i\omega_n t} \quad (20)$$

The pressure and axial velocity used here must each be physically real-valued, so that the series coefficients satisfy the conjugate identity for negative frequencies:

$$\hat{p}(L; -\omega_n) = \hat{p}^*(L; \omega_n) \quad (21)$$

and

$$\hat{u}(L; -\omega_n) = \hat{u}^*(L; \omega_n) \quad (22)$$

where the superscript $*$ denotes the complex conjugate. These coefficients are integrals (over a single period) of the product of time functions and the complex exponential $e^{-i\omega t}$:

$$\hat{p}(L; \omega_n) = \frac{1}{T} \int_{t-T}^t e^{-i\omega_n \tau} \tilde{p}(L, \tau) d\tau \quad (23)$$

and

$$\hat{u}(L; \omega_n) = \frac{1}{T} \int_{t-T}^t e^{-i\omega_n \tau} \tilde{u}(L, \tau) d\tau \quad (24)$$

In this definition of the coefficient, the choice of t is unimportant; however, the definition has the physical implication that the coefficient depends on the time period that immediately preceeds the present t . The band-limited pressure and normal velocity functions considered here are not restricted to zero mean values, so that the zero-frequency coefficient is not necessarily zero:

$$\hat{p}(L; \omega_0) \neq 0 \quad (25)$$

and

$$\hat{u}(L; \omega_0) \neq 0 \quad (26)$$

This requirement is necessary to accommodate nonlinear effects. Note that only $(N + 1)$ complex constants are needed to represent each fluctuating function $\tilde{p}(L, t)$ and $\tilde{u}(L, t)$. Often, the integer N is taken to be some integer power M of 2 to take advantage of the FFT:

$$N = 2^M \quad (27)$$

In practical problems, M may range from 5 to 10, so that N would range from 32 to 1,024. (These numbers are only typical values.)

The boundary conditions utilized here use generalized forms of impedance and admittance. The elementary scalar forms of these relations in the frequency-domain are

$$\hat{p}(L; \omega_n) = \hat{Z}(\omega_n) \hat{u}(L; \omega_n) \quad (28)$$

$$\hat{u}(L; \omega_n) = \hat{\beta}(\omega_n) \hat{p}(L; \omega_n) \quad (29)$$

where $\hat{Z}(\omega_n)$ is the impedance and $\hat{\beta}(\omega_n)$ is the admittance. Values of $\hat{Z}(\omega_n)$ and $\hat{\beta}(\omega_n)$ that correspond to outgoing acoustic waves are obtained from standard frequency-domain analyses (reference [7]) The time-domain forms of equations (28) and (29) are given by convolution integrals:

$$\tilde{p}(L, t) = \int_{t-T}^t Z(t - \tau) \tilde{u}(L, \tau) d\tau = \langle Z * \tilde{u} \rangle \quad (30)$$

$$\tilde{u}(L, t) = \int_{t-T}^t \beta(t - \tau) \tilde{p}(L, \tau) d\tau = \langle \beta * \tilde{p} \rangle \quad (31)$$

The time-domain, or temporal, impedance and admittance are functions of the time delay $t - \tau$, as in equation (19):

$$Z(t - \tau) = \frac{1}{T} \sum_{n=-N}^N \hat{Z}(\omega_n) e^{i\omega_n(t-\tau)} \quad (32)$$

$$\beta(t - \tau) = \frac{1}{T} \sum_{n=-N}^N \hat{\beta}(\omega_n) e^{i\omega_n(t-\tau)} \quad (33)$$

Either equation (30) or (31) is a time-domain radiation condition to be applied at $x = L$. Results presented in this paper were obtained with the impedance form of the radiation condition (equation (30)). In time-domain computations, the impedance or admittance function, defined by either equation (32) or (33) is tabulated and held for use by the computational algorithm. If the computation proceeds in uniform time increments, direct table lookups supply the requested values at minimal cost. We assume here that the preliminary computation produces a table with acceptably fine resolution, such that direct lookup supplies the needed value of the impedance or admittance. Uneven time increments involve additional computation at each time step, evaluation of the series at each point, or additional preliminary computations to produce an enlarged preliminary tabulation that is suitable for interpolation by some simple formula.

A similar argument holds for the acoustic pressure or axial velocity required to perform the time integration in equations (30) and (31). One of these variables must be computed by using the computational algorithm and then held for use for one period; the other is computed from radiation condition equation (30) or (31). Because the integrand of either radiation condition is known only at discrete time increments, numerical integration is required to implement the boundary condition. The advantage of the boundary-condition formulation that is presented here is the generality that it affords. The convolution equations provide a direct means for extending the time-domain boundary condition in one space dimension to any number of spatial dimensions and to ducts with acoustically treated walls and arbitrary sources. This extension requires the use of the frequency-domain nonlocal nodal impedance matrix operators. These matrix impedance operators have been shown to be an accurate and effective computational boundary condition in duct acoustics (references [7, 8]).

4 The Numerical Method

Now that we have specified initial and boundary conditions for the Euler system (equation (1)), we focus on a numerical solution technique. One specific algorithm that has gained wide acceptance for solving time-dependent problems in fluid dynamics is MacCormack's predictor-corrector scheme (reference [9]). This algorithm is used here to integrate the Euler system, coupled with the initial, inflow, and radiation conditions to a periodic state. We describe the method here for the interested reader.

To apply MacCormack's method to the Euler system, the continuum region of interest (x, t) , is replaced with a discrete finite-difference mesh (x_j, t_n) as shown in figure 2. Thus, in the finite-difference mesh, we denote the pressure at grid point (x_j, t_n) by $p_{j,n}$. The finite-difference mesh is assumed to contain NX evenly spaced points in the axial direction, as shown. The grid spacing in the x and t direction is denoted by Δx and Δt , respectively. The grid spacing in the t direction (i.e., Δt) is not necessarily evenly spaced. MacCormack's solution of equation (1) within the grid in figure 2 takes the form of a predictor-corrector technique by using forward differences on the predictor step and backward differences on the corrector step. Although the differences are first-order accurate in each step, the overall solution is second-order accurate in both space and time. Because MacCormack's time-marching

algorithm is explicit, roundoff error can grow in an unbounded manner and destroy the solution if the Cauchy-Friedrichs-Lewy (CFL) criterion is not satisfied. The physical significance of the CFL criterion is that the time step Δt must be, at most, equal to the time required for a sound wave to propagate between two adjacent grid points. The criterion gives the following time step restriction (reference [9]):

$$\Delta t = \sigma_t (\Delta t)_{max} \quad (34)$$

where $(\Delta t)_{max}$ is the maximum value of $\frac{\Delta x}{|u|+c}$ within the computational domain, and σ_t is a positive constant less than unity.

The following is a summary of the steps involved to advance the solution forward in time.

1. Choose a coordinate grid Δx that is sufficiently fine to resolve all spatial gradients in the duct.
2. Beginning with the initial condition, apply equation (34) at each grid point to determine a minimum time step Δt for the integration.
3. Beginning with the known solution at t , integrate the Euler system (equation (1)) by using MacCormack's scheme at all interior points to advance the interior solution to the next time step $t + \Delta t$.
4. Special care is required to advance the solution in time along the inflow and outflow boundary. Along these boundaries, some conditions are prescribed; others must be obtained from the compatibility conditions of the Euler system. Along the inflow boundary $x = 0$, the two inflow conditions and the axial momentum equation are used to advance the solution in time. To compute the inflow pressure, we use the discrete form of the known source condition (equation (9)):

$$p_{1,n+1} = P_0 + g_{n+1} \quad (35)$$

The homoentropic condition (equation (10)) now gives the inflow density from the known interior solution and the inflow pressure obtained from (equation (35))

$$\rho_{1,n+1} = \rho_{2,n+1} + \frac{p_{1,n+1} - p_{2,n+1}}{c_0^2} \quad (36)$$

To advance the inflow axial velocity to the next time step, we integrate the axial momentum equation (i.e., the second component of equation (1)) in time along the inflow boundary with MacCormack's scheme. This integration is performed by using forward differences for all axial gradients in the equation. Along the outflow boundary, the density ρ and axial velocity u are advanced in time by integrating the first two components of equation (1) forward in time with MacCormack's scheme. Backward differences are used to approximate all axial gradients in the integration. The radiation condition (equation (30)) provides the necessary condition for obtaining the outflow pressure p :

$$p_{NX,n+1} = P_0 + \langle Z * \tilde{u}_{NX} \rangle \quad (37)$$

The time integration in (equation 37)) is performed numerically. Axial velocity values are held by the algorithm for one time period, and cubic spline interpolation is applied to perform this numerical integration.

5. Continue to advance the solution in time until a periodic state is achieved.

5 Results and Discussion

A computer code that implements the boundary condition derived in this paper has been developed and programmed to run on a DEC-Alpha work station and a Cray computer. Results presented in this section were obtained with the underlying objective of comparing the periodic waveform obtained from the boundary condition with the exact solution for a range of source and initial conditions. The grid is uniformly spaced with 51 points (i.e., $NX = 51$) over the length of the duct L . All results are calculated for an ambient base state in which $P_0 = 101325$, $c_0 = 343$, $\rho_0 = 1.2$, and $L = \frac{\pi c_0}{1420}$. (throughout this work, the international units of measure are used). The sound source oscillates sinusoidally at a fundamental frequency of $\frac{1100}{\pi}$ Hz (i.e., $\omega = 2200$). Uniform time steps are used and the CFL number is $\frac{1}{20}$ of its maximum value (i.e., $\sigma_t = 0.05$). This time step is used because, in addition to satisfying the CFL criteria, it is small enough to provide accurate numerical data for evaluating the convolution integral in the radiation boundary condition (see equations (30) and (31)). The accuracy of the numerical solution at several points in the duct was investigated; and as expected, these results were more accurate than those results computed at the outflow boundary. Therefore, to limit the number of graphs, results are presented only at the outflow boundary $x = L$.

The frequency-domain impedance $\hat{Z}(\omega_n)$, which corresponds to outgoing plane waves, is the characteristic impedance of the medium for the current one-dimensional problem:

$$\hat{Z}(\omega_n) = \rho_0 c_0 \quad (38)$$

Thus, in one space dimension, the temporal impedance (equation (32)) reduces to the product of the characteristic impedance of the medium $\rho_0 c_0$ and a dirac delta function $\sigma_N(t - \tau)$:

$$Z(t - \tau) = \rho_0 c_0 \sigma_N(t - \tau) \quad (39)$$

$$\sigma_N(t - \tau) = \frac{1}{T} \sum_{n=-N}^N e^{in\omega(t-\tau)} = \frac{1}{T} \left[1 + 2 \sum_{n=1}^N \cos n\omega(t - \tau) \right] = \frac{1}{T} \left[\frac{\sin \frac{2N+1}{2}\omega(t - \tau)}{\sin \frac{\omega(t-\tau)}{2}} \right] \quad (40)$$

Although the upper limit of summation N would be infinity, for a general wave the assumption of a band-limited periodic wave allows N to be truncated to a finite integer, which implies that the smallest acceptable value of N depends upon the bandwidth at the source. If the initial condition is transient free and the sound source is a pure tone, then a one term expansion (i.e., $N = 1$) of the Dirac delta function is sufficient. However, initial conditions with significant transients require a much larger value of N before the temporal impedance can be accurately represented.

Note that because the temporal impedance $Z(t - \tau)$ is a Dirac delta function in one space dimension, the integration in equation (30) could be performed analytically by using the shifting property of the Dirac delta function:

$$\tilde{p}(L, t) = \rho_0 c_0 \tilde{u}(L, t) \quad (41)$$

Equation (41) can be rewritten in terms of p and u to yield

$$p(L, t) - P_0 = \rho_0 c_0 u(L, t) \quad (42)$$

Equation (42) can be differentiated with respects to time to recover the linearized form of both the Hedstrom(reference [2]) and the one-dimensional Thompson(reference [3]) boundary condition:

$$\frac{\partial p(L, t)}{\partial t} - \rho_0 c_0 \frac{\partial u(L, t)}{\partial t} = 0 \quad (43)$$

Unfortunately, in higher dimensional problems the temporal impedance will not be a Dirac delta function, and this integration must be carried out numerically. It is for this reason that sample calculations are presented using the exact analytical result (equation (41)) and results from the numerical integration equation (30).

5.1 Results for pure-tone source

In the first sample problem the source is a pure tone:

$$g(t) = A \sin(\omega t) \quad (44)$$

$$A = \epsilon P_0 \quad (45)$$

where the parameter ϵ must be considerably less than unity for the solution to exhibit linear behavior. Results presented in this section were calculated with $\epsilon = 10^{-3}$. The exact periodic acoustic solution, without reflections, can be computed from linearized acoustic theory:

$$p_{exact}(x, t) = A \sin(\omega t - \frac{\omega x}{c_0}) \quad (46)$$

This exact analytical solution is used as a test case to verify the accuracy of the radiation condition. We introduce the normalized error function $E(x, t)$ conveniently defined as the difference between the exact solution and the MacCormack solution:

$$E(x, t) = \frac{p_{exact}(x, t) - p_{MacCormack}(x, t)}{A} \quad (47)$$

The MacCormack solution contains error that is attributable to both discretization and computer roundoff as well as to initial transients that are reflected and not absorbed by the radiation condition. For a sufficiently fine grid, that is free of initial transients, the distribution of error $E(x, t)$ will be considerably less than unity at the periodic state. Further, if the grid is sufficiently fine, then $E(x, t)$ provides a measure of the initial transients that cannot pass through the radiation boundary.

Graphs of the normalized outflow error $E(L, t)$ for $N = 2$ and $N = 60$ (see equation (40)) are shown in figure 3. The curve that is labeled exact integration is obtained by using equation (41) as the radiation condition for MacCormack's scheme. The initial condition that is used to generate each curve is transient free. The transient-free initial condition is

obtained by using $t = 0$ in equation (46). Because the initial data are transient free, $E(x, t)$ contains the effects of discretization and roundoff error only. The curve that corresponds to the smallest number of terms in the Dirac delta function expansion (i.e., $N = 2$) has the largest error. However, on this scale the effects of these errors are small for the chosen grid since they are less than 2 percent of the amplitude of the periodic state. Furthermore, when $N = 60$ the discretization and roundoff errors are just as small in magnitude as those obtained from the exact integration. Graphs of the normalized outflow acoustic pressure that is computed from the boundary conditions are compared with the exact periodic solution in figure 4. The solid curve denotes the exact periodic solution from linear theory; the broken lines denote the solution obtained with the temporal impedance radiation condition. The acoustic pressure has been normalized with the amplitude A and the physical time t with the fundamental period of the source $T = \frac{2\pi}{\omega}$. Each curve collapses onto the curve for the exact periodic solution.

The next example is presented to specifically show the effects of the radiation condition on initial transients. The result in figure 5 are similar to those in figure 3, when the system is initiated from rest (see equations (6)-(8)). This initial condition generates significant transients, which must be eliminated from the solution domain by the radiation condition before a periodic state can be achieved. Because the discretization and roundoff error introduced by the current grid is small in comparison with the periodic amplitude (see figure 3), the error plotted in figure 5 can be attributed to transient effects. Approximately 0.8 of one period (i.e., $t = 0.8T$) is required before the initial transient reaches the outflow boundary. The effect of the number of terms N on the transient is apparent. When $N = 2$, the normalized error is unacceptable and grows in time. Thus, for a two-term expansion the transient wave does not pass rapidly out of the solution domain. However, when $N = 60$ the temporal impedance is more accurately represented, and a much larger portion of the initial transient is eliminated by the radiation condition than is eliminated when $N = 2$. This difference is especially true for large times. Figure 5 clearly shows that the best results are obtained when the time integration in the radiation condition is performed exactly. Furthermore, when exact integration is used the transient wave is transparent to the radiation boundary.

Graphs of the outflow acoustic pressure which is computed by using the initial condition with significant transients, are compared with the exact periodic solution in figure 6. Discrepancies between the exact and numerically computed curves in the figure are due to transient effects. Results calculated with $N = 2$ are not accurate. When $N = 60$, the initial transient is passed rapidly out of the solution domain by the temporal impedance, as expected. Superior results are obtained if the time integration in the radiation condition is performed exactly. After four time periods, the periodic solution obtained from each curve is accurate, except for the curve that corresponds to $N = 2$.

5.2 Results for Broadband Source

In the final sample problem the source is a multitone source:

$$g(t) = A[\sin(\omega t) + \sin(2\omega t)] \quad (48)$$

where the amplitude $A = 10^{-3}P_0$ and the fundamental circular frequency ω is 2200 rad/s. Sources of this type are typical of those generated by ducted fans. The outflow acoustic

pressure is plotted in figure 7. The initial condition used to generate the results in this figure contains significant transients (i.e., the disturbance was initialized from rest), and a 60-term expansion is used to represent the Dirac delta function. Results computed with the time-domain radiation condition agree extremely well with the exact results from linear theory. No evidence is found that indicates reflections of the initial transient on this scale.

6 Conclusions

A general theory for deriving time-domain nonlocal, nonreflecting boundary conditions for duct acoustics has been presented. The formulation is presented here in one space dimension and time; however, this formulation can be extended in a straightforward manner to variable-area, higher dimensional, and acoustically treated ducts. The temporal operators for the time domain are shown to be convolution integrals of known frequency-domain operators. Accuracy of the time-domain condition has been tested by applying a MacCormack integration to the Euler equations in one space dimension and time. The time limit for the time integration was arbitrarily set at 10 source periods to control computational cost. The MacCormack integration utilizes the boundary condition at an artificial boundary to limit the computational space and prevent spurious reflections. Results of this study show that the boundary conditions are extremely effective on both pure tones and broadband sources. Results obtained for a variety of initial conditions compared extremely well with known nonreflecting solutions after integrating the differential equations for no more than four source periods. Results show that a large number of terms are required in the temporal impedance operator when a significant amount of transients exist in the initial condition. When significant amounts of transients exist time steps that are smaller than the size established by the maximum CFL number must be taken in the numerical scheme. The smaller time steps are necessary to accurately evaluate the convolution integral in the radiation boundary condition.

The success of the temporal boundary conditions motivates their extension to higher dimensional and acoustically treated ducts. In higher dimensions, the boundary condition is more complex and involves a much greater computational effort. For example, the boundary condition will be a matrix convolution operator in two dimensions and a tensor convolution operator in three dimensions.

Although a major purpose of the boundary condition is to improve accuracy and reduce the computational effort necessary for the solution of duct problems in large-volume domains, some point may be reached at which the added boundary-condition complexity, no longer results in a net reduction of computational effort when the computational volume is reduced. In this case, the major advantage of the boundary condition is its ability to account for the effects of sound-absorbing materials.

References

- [1] Engquist, Bjorn; and Majda, Andrew.: Absorbing Boundary Conditions for the Numerical Simulation of Waves. *Mathematics of Computations*, vol. 31, 1977, pp. 629–651.

- [2] Hedstrom, G.W.: Nonreflecting Boundary Conditions for Nonlinear Hyperbolic Systems. *Journal of Computational Physics*, vol. 30, 1979. pp. 222-237.
- [3] Thompson, Kelvin W.: Time Dependent Boundary Conditions for Hyperbolic Systems. *Journal of Computational Physics*, vol. 68, 1987, pp. 1-28.
- [4] Bayless, A.; and Turkel, E.: Radiation Boundary Conditions for Acoustic and Elastic Wave Calculations. *Communications on Pure and Applied Mathematics*, vol. 32, 1979 pp. 312.
- [5] Giles, M. B.: Nonreflecting Boundary Conditions for Euler Equation Calculations. AIAA Paper 89-1912, 1989.
- [6] Watson, Willie R.; and Myers, M. K.: Time Dependent Inflow-Outflow Boundary Conditions for 2-D Acoustic Systems. *AIAA Journal*, vol. 29, no. 9, Sept. 1991, pp. 1383-1389.
- [7] Zorumski, W. E.; Watson, W. R.; and Hodge, S. L.: A Nonlocal Computational Boundary Conditions for Duct Acoustics. *Journal of Computational Acoustics*, vol. 3, No. 1, 1995, pp. 15-26.
- [8] Watson, W. R.; Zorumski, W. E; and Hodge, S. L.: Evaluation of Several Non-reflecting Boundary Conditions for Duct Acoustics. *Journal of Computational Acoustics*, vol. 3, no. 4, 1995, pp. 327-342.
- [9] Anderson, D. A.; Tannehill, J. C.; and Pletcher, R. H.: *Computational Fluid Mechanics and Heat Transfer*, McGraw Hill, 1984.

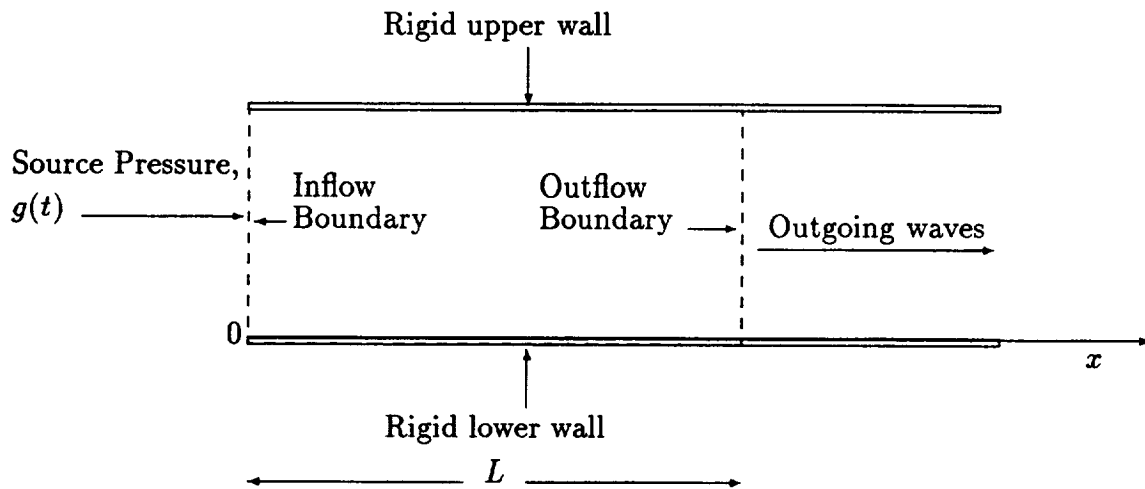


Figure 1: Infinitely long duct and coordinate system.

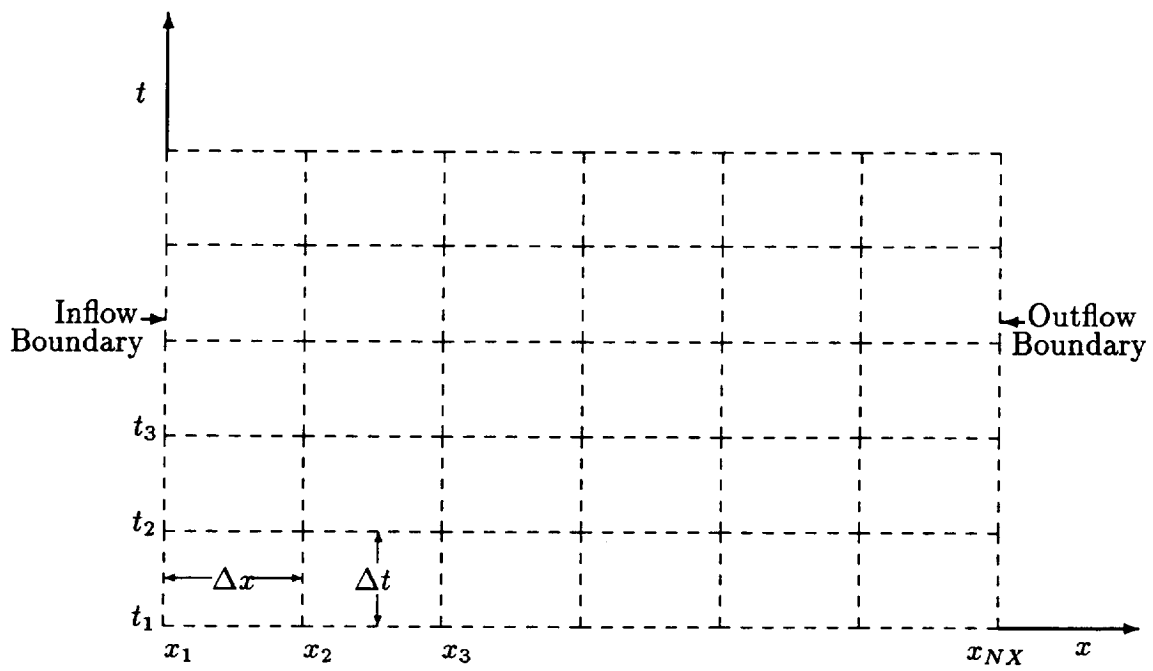


Figure 2: Continuous (x, t) and discrete domain (x_j, t_n) .

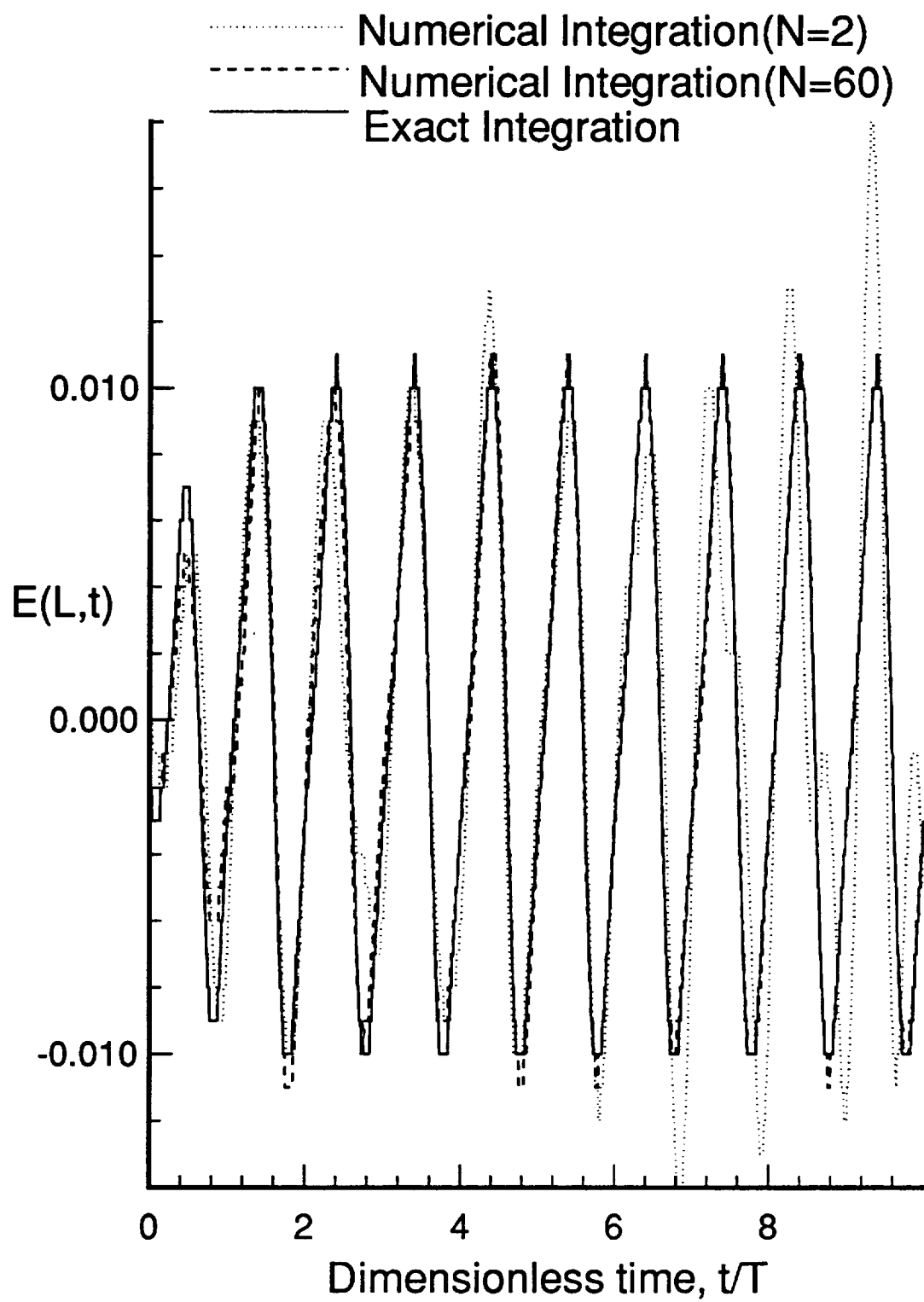


Figure 3: Error function for pure-tone source (transient free).

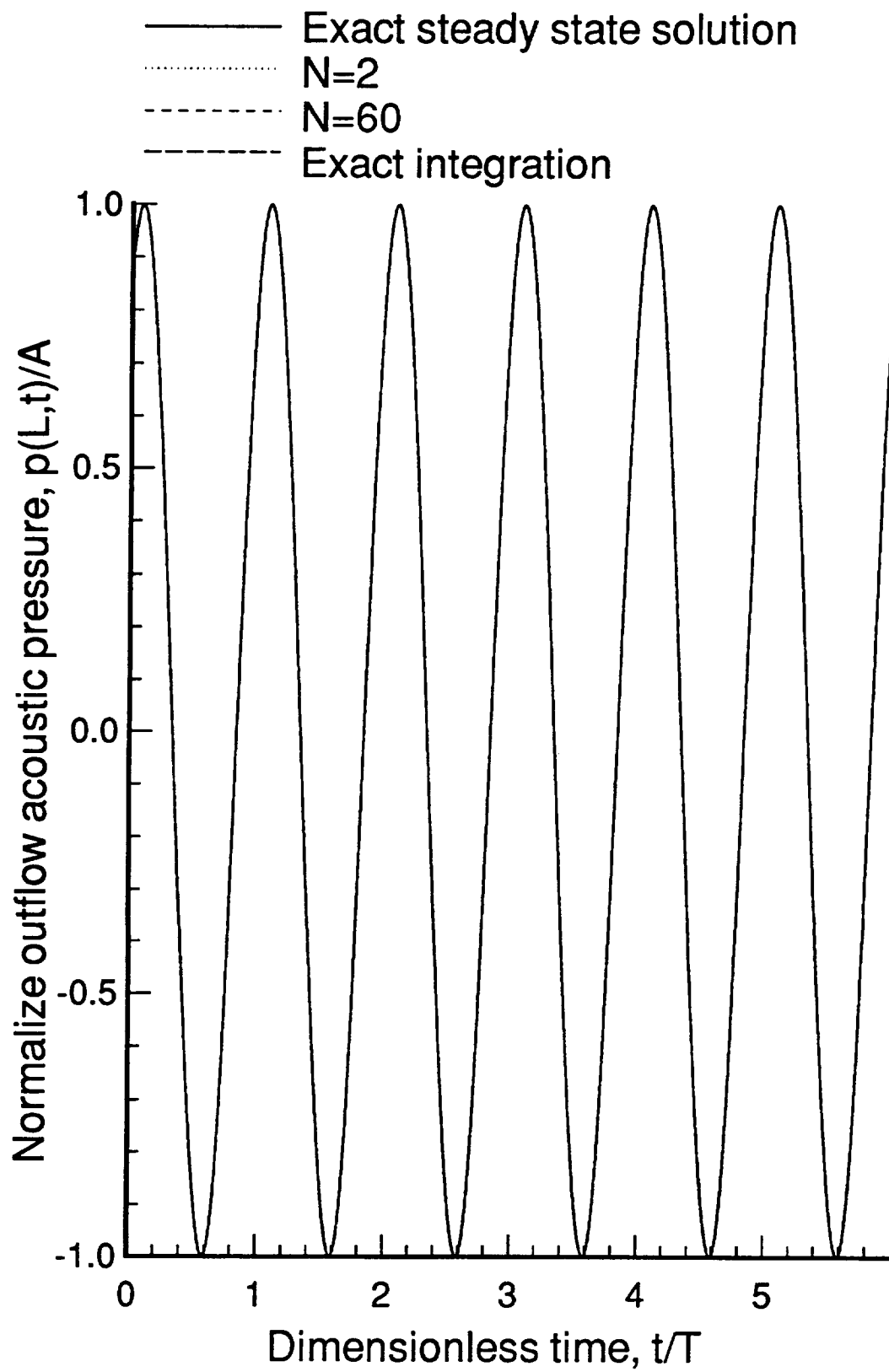


Figure 4: Normalized acoustic pressure for pure-tone source (transient free).

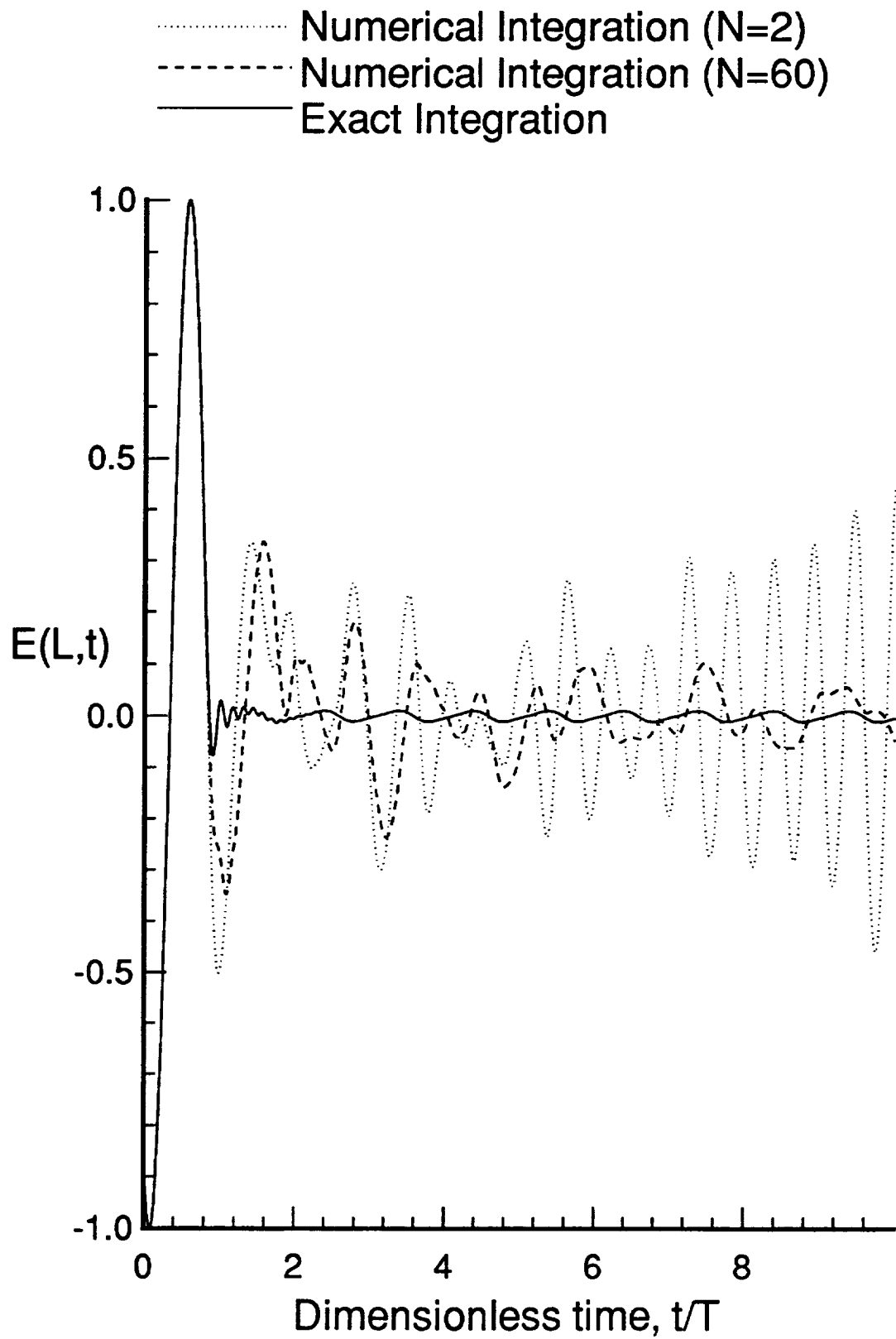


Figure 5: Error function for pure-tone source (significant transients).

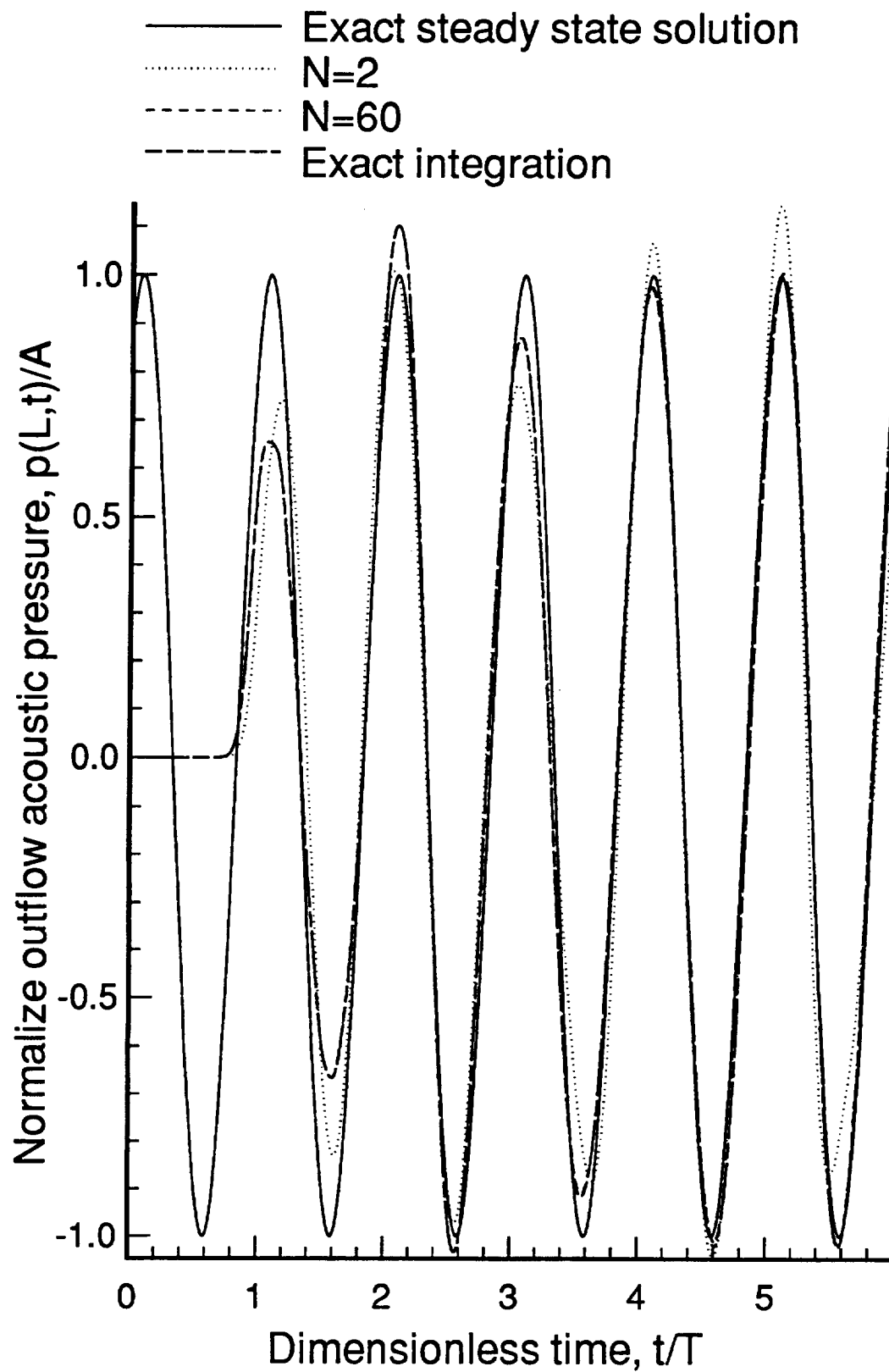


Figure 6: Normalized acoustic pressure for pure-tone source (significant transients).

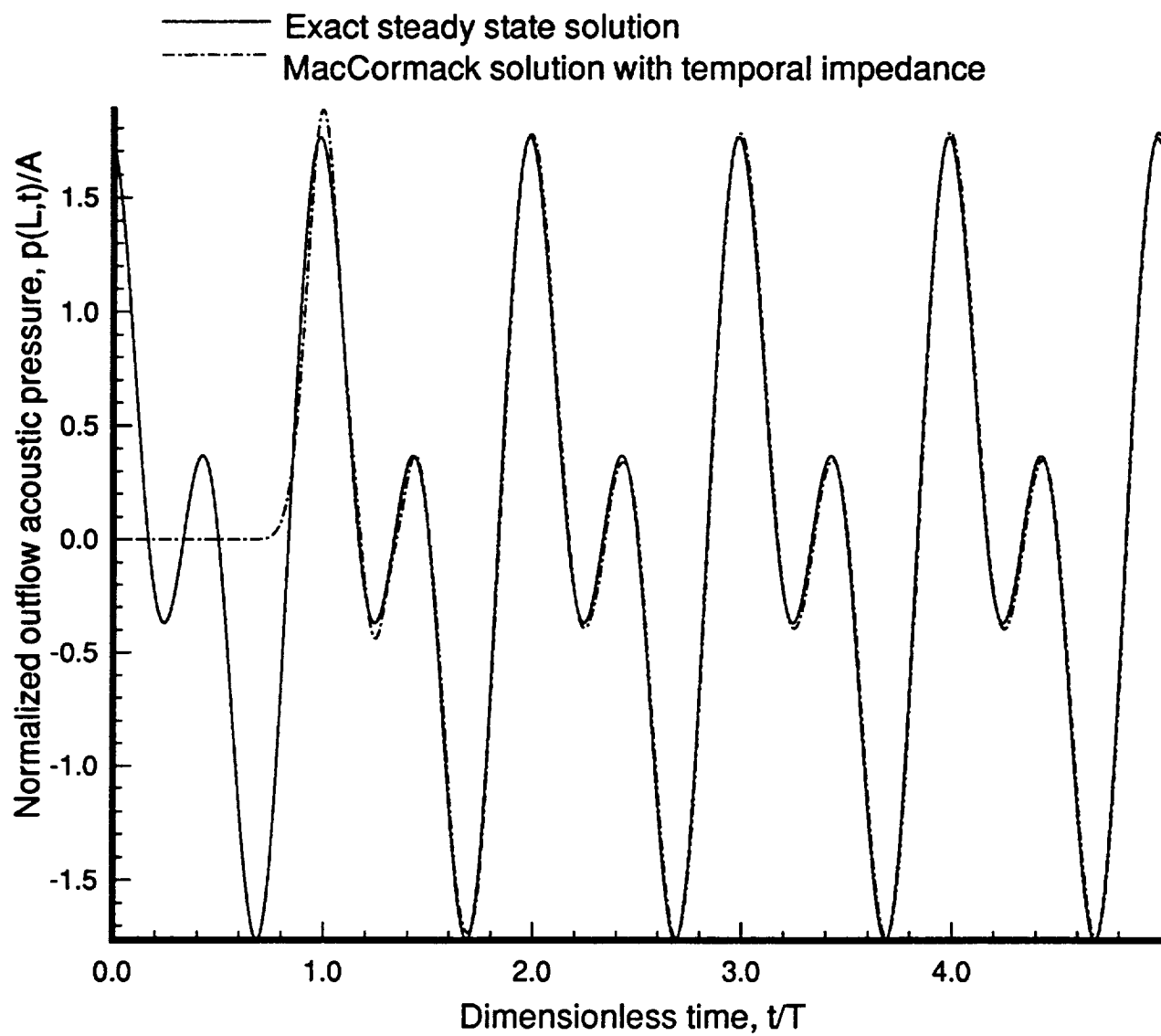


Figure 7: Normalized acoustic pressure for multitone source (significant transients).

REPORT DOCUMENTATION PAGE			Form Approved OMB No. 0704-0188	
Public reporting burden for this collection of information is estimated to average 1 hour per response, including the time for reviewing instructions, searching existing data sources, gathering and maintaining the data needed, and completing and reviewing the collection of information. Send comments regarding this burden estimate or any other aspect of this collection of information, including suggestions for reducing this burden, to Washington Headquarters Services, Directorate for Information Operations and Reports, 1215 Jefferson Davis Highway, Suite 1204, Arlington, VA 22202-4302, and to the Office of Management and Budget, Paperwork Reduction Project (0704-0188), Washington, DC 20503.				
1. AGENCY USE ONLY (Leave blank)		2. REPORT DATE June 1996		3. REPORT TYPE AND DATES COVERED Technical Memorandum
4. TITLE AND SUBTITLE Periodic Time Domain Nonlocal Nonreflecting Boundary Conditions for Duct Acoustics			5. FUNDING NUMBERS 505-59-52	
6. AUTHOR(S) Willie R. Watson and William E. Zorumski				
7. PERFORMING ORGANIZATION NAME(S) AND ADDRESS(ES) NASA Langley Research Center Hampton, VA 23681-0001			8. PERFORMING ORGANIZATION REPORT NUMBER	
9. SPONSORING / MONITORING AGENCY NAME(S) AND ADDRESS(ES) National Aeronautics and Space Administration Washington, DC 20546-0001			10. SPONSORING / MONITORING AGENCY REPORT NUMBER NASA TM-110230	
11. SUPPLEMENTARY NOTES Watson and Zorumski: Langley Research Center Hampton, VA				
12a. DISTRIBUTION / AVAILABILITY STATEMENT Unclassified - Unlimited Subject Category 71 Availability: NASA CASI, (301) 621-0390			12b. DISTRIBUTION CODE	
13. ABSTRACT (Maximum 200 words) Periodic time-domain boundary conditions are formulated for direct numerical simulation of acoustic waves in ducts without flow. Well-developed frequency-domain boundary conditions are transformed into the time domain. The formulation is presented here in one space dimension and time; however, this formulation has an advantage in that its extension to variable-area, higher dimensional, and acoustically treated ducts is rigorous and straightforward. The boundary condition simulates a nonreflecting wave field in an infinite uniform duct and is implemented by impulse-response operators that are applied at the boundary of the computational domain. These operators are generated by convolution integrals of the corresponding frequency-domain operators. The acoustic solution is obtained by advancing the Euler equations to a periodic state with the MacCormack scheme. The MacCormack scheme utilizes the boundary condition to limit the computational space and preserve the radiation boundary condition. The success of the boundary condition is attributed to the fact that it is nonreflecting to periodic acoustic waves. In addition, transient waves can pass rapidly out of the solution domain. The boundary condition is tested for a pure tone and a multitone source in a linear setting. The effects of various initial conditions are assessed. Computational solutions with the boundary condition are consistent with the known solutions for nonreflecting wave fields in an infinite uniform duct.				
14. SUBJECT TERMS Time domain boundary conditions, non-reflecting boundary conditions, nonlocal boundary conditions and Euler's Equations			15. NUMBER OF PAGES 19	
			16. PRICE CODE A03	
17. SECURITY CLASSIFICATION OF REPORT Unclassified	18. SECURITY CLASSIFICATION OF THIS PAGE Unclassified	19. SECURITY CLASSIFICATION OF ABSTRACT	20. LIMITATION OF ABSTRACT	